



# IoT-Enabled Distributed Detection of a Nuclear Radioactive Source via Generalized Score Tests

Giampaolo Bovenzi<sup>1</sup>, Domenico Ciuonzo<sup>2(✉)</sup>, Valerio Persico<sup>1,2</sup>,  
Antonio Pescapè<sup>1,2</sup>, and Pierluigi Salvo Rossi<sup>3</sup>

<sup>1</sup> University of Naples “Federico II”, Naples, Italy  
giampaolo.bovenzi@gmail.com, {valerio.persico,pescape}@unina.it

<sup>2</sup> Network Measurement and Monitoring (NM2), Naples, Italy  
domenico.ciuonzo@ieee.org

<sup>3</sup> Kongsberg Digital AS, Trondheim, Norway  
salvorossi@ieee.org

**Abstract.** A decentralized detection method is proposed for revealing a radioactive nuclear source with unknown intensity and at unknown location, using a number of cheap radiation counters, to ensure public safety in smart cities. In the source present case, sensors nodes record an (unknown) emitted Poisson-distributed radiation count with a rate decreasing with the sensor-source distance (which is unknown), buried in a known Poisson background and Gaussian measurement noise. To model energy-constrained operations usually encountered in an Internet of Things (IoT) scenario, local one-bit quantizations are made at each sensor over a period of time. The sensor bits are collected via error-prone binary symmetric channels by the Fusion Center (FC), which has the task of achieving a better global inference. The considered model leads to a one-sided test with parameters of nuisance (i.e., the source position) observable solely in the case of  $\mathcal{H}_1$  hypothesis. Aiming at reducing the higher complexity requirements induced by the generalized likelihood ratio test, Davies’ framework is exploited to design a generalized form of the locally optimum detection test and an optimization of sensor thresholds (resorting to a heuristic principle) is proposed. Simulation results verify the proposed approach.

**Keywords:** CBRN sensors · Data fusion · Distributed detection  
IoT · Public safety · Smart cities · Wireless Sensor Networks

## 1 Introduction

Almost 70% of the population of the world ( $\approx$  six billion people) is expected to live in cities (and, also, neighboring regions) in next thirty years. So, the need for smart(er) cities, using information and communication technologies, is becoming an imperative to make their services and monitoring more efficient, interactive and aware, and keep them on the track to flourish as platforms enabling

well-being from economic, environmental and social viewpoints. The smart city concept is fostered (also from a technological standpoint) by the Internet of Things (IoT) paradigm, representing an unprecedented Internet evolution into a pervasive network of interconnected entities that (a) collects data from the environment, (b) allows interaction with the physical world and (c) uses Internet infrastructure to furnish services for data analytics, information transfer, and applications usage [1].

Wireless Sensor Networks (WSNs) constitute the actuation/sensing arm of the IoT and are able to naturally permeate the urban infrastructure, thanks to their flexibility, reduced costs, and applicability to several domains [2]. Their collected information is expected to be shared across diverse applications and tools to build-up a shared operating city “picture”, representing the milestone to enable different smart city applications. Among those, *public safety and security* is of critical and paramount importance, and innovations in the IoT will likely convert into safety improvement of citizens. Indeed, nowadays crowded places are subject to increasingly high risk and traditional security approaches, such as searches and checkpoints, have become obsolete while altering public experience and people lifestyle. Then, the development of an environment that presents counter-terrorism to both *cyber* and *physical* aspects of urban systems as a “built-in” feature is the stepping stone toward safety-resilient cities, and represents the hope of ensuring improved security in both effective and acceptable ways [3].

For the mentioned reasons, one key task is represented by detection of radioactive sources using a WSN made of massively-deployed and low-cost sensors, usually Geiger–Muller counters, in densely-populated areas. Indeed, detection of radioactive emissions from nuclear materials constitutes an important objective, given the increasing hazards from potential terrorist activities, e.g. the recognition of *dirty bombs*, apparently-common explosive devices with release of radioactive isotopes upon explosion (such as Caesium-137, obtainable with considerable ease). Therefore, a relevant scenario is to *proactively* detect radiations having a low-level from this type of sources when they are carried or stored and before they are employed, or, *reactively* detect traces of radiation and quantify their extent after ordinary explosions, ensuring awareness and protection of first responders against the low-level (yet highly hazardous) radiation [4]. Indeed, in both cases, the radiation levels are as low as to be confused with “ordinary” fluctuations of the background radiation and therefore sophisticated algorithmic solutions are required. The benefits (as well as the costs) of using a set of radiation detectors (instead of a single one) for revealing a radioactive source have been investigated and evaluated in [5, 6].

For the mentioned reasons, several approaches have been devised in the literature for WSN-based detection of nuclear sources. For example, in [7] the authors consider detection of a single source modeled as time-inhomogeneous process following a Poisson law, embedded in the background radiation using full-precision measurements from a network of nodes, assuming all the parameters *known*. The same setup is studied in [8] to obtain Chernoff bounds for the missed detection and false alarm probabilities, which are employed to design an

optimal motion control approach to drive the sensors, and to obtain the optimal values of the threshold for the decision test, versus the sensor and source trajectories. On the other hand, in [9] the problem of jointly estimating an unknown number of sources and the corresponding locations and intensities is tackled, and two different approaches are proposed therein. The first is based on the generalized maximum likelihood rule, whereas the second approach resorts to parameter estimation in the Bayesian framework (via Monte Carlo integration). Similarly, in [10] the same task is approached via a Bayesian framework and, specifically, source detection is tackled as a model order selection problem where partial Bayes factors (whose efficient computation is accomplished via importance sampling using progressive correction) are employed to weight each potential befitting model. Later, in [11] a search lead by the information gain, including a Bayesian estimator in sequential form coupled with a sensor/observer control unit, is developed and successfully compared to a uniform search along a predefined path. The control unit leads the observers to migrate to new locations and acquires measurements that maximize the information gain in the Renyi divergence sense. Unfortunately, all the above works *require full-precision reporting*, which may be unsuitable in a realistic IoT scenario where inexpensive nodes are usually employed.

Indeed, stringent bandwidth and energy constraints hinder full-precision reporting and, as a consequence, each sensor usually provides one bit to the Fusion Center (FC) regarding the inferred hypothesis. In such a case, the optimal sensor-individual decision procedure (from both Bayesian and Neyman-Pearson standpoints) corresponds to the local Likelihood-Ratio Test (LRT) being quantized into one-bit [12, 13]. Unfortunately, the design of quantization thresholds has an exponential complexity and, equally important, sensor LRT evaluation is precluded by ignorance of the parameters of the source to be detected [14]. Hence, the bit reported is either the outcome of a quantization made via a “dumb” rationale [15, 16] or exemplifies the inferred binary-valued event (obtained via a sub-optimal detection statistic [17]). In both situations, FC gathers sensors bits and fuses them via a wisely-designed rule to improve (single-)sensor detection capability. Under the assumption of conditional independence, the optimum decision statistic is a weighted sum of decisions, *with weights being function of all the parameters specifying the unknown radiation source* [2]. Then, simple fusion strategies, such as the well-known counting rule or based on simplified design assumptions (for the sensing model), have been initially devised to circumvent such unavailability [18–21]. For example, referring to the radioactive source detection problem, in [22] a two-step approach is proposed, based on (i) geometric sensor localization methods employed to estimate the location and strength of the source and (ii) a sensor-specific test via the sequential probability ratio based on estimated parameters and new measurements to decide individually the source presence. Finally, decisions from different sensors are finally combined through a majority voting rationale. Similarly, in [23] one- and two-sided Wald-statistics at each sensor are adopted, whereas at the FC the counting rule is applied to combine the sensors’ hard decisions.

On the other hand, in [24], the authors derive a test for fusing of correlated decisions and obtaining the sensor (optimal) thresholds for the case of two sensors via *copula-theory*, while a counterpart for the general case of  $N$  sensors is provided in [25]. Differently, in [26] a hierarchical Poisson-Gamma law is used to model the probability mass function of the received sensors' counts, and the nodes are assumed to adopt threshold-based (viz. deterministic) binary quantizers sending a decision vector during time to the FC for improved decision-making. Resorting to the hypothesized sensing model, the authors propose a Generalized Likelihood Ratio Test (GLRT) based on a Maximum Likelihood Estimator (MLE) in *constrained form* as the relevant FC decision statistic. Indeed, when the model is parametrically specified, the FC is in charge to tackle a composite test of hypotheses and the GLRT is usually taken as the natural design solution [27]. Indeed, GLRT-based fusion of quantized data has been extensively studied in WSN literature [16, 28, 29] for target detection in the following cases: (i) a cooperative target with unknown location, (ii) an cooperative target modelled by observation coefficients assumed known, and (iii) an unknown source at unknown position. The last scenario represents the most interesting and suitable for nuclear source detection, as it requires the *least source knowledge*. A different approach is instead pursued in [30], where a Locally Optimum Detection (LOD) scheme is proposed for detecting a radioactive weak source embedded in background clutter. Based on the latter rationale, a decentralized approach, exploiting the Alternating Direction Method of Multipliers (ADMM), is developed for a totally-distributed WSN (no FC), and a (low-overhead) ADMM algorithm robust to attacks, consisting in data falsification, demonstrated. Unfortunately, although appealing (as they attempt to solve the resulting composite hypothesis testing), the aforementioned two methods do not take explicitly into account source location when formulating the hypothesis testing.

Accordingly, in this paper we study detection, in decentralized fashion, of a nuclear radioactive source (i) having a spatially-dependent signature, (ii) with unknown location and (iii) with emitted intensity modeled as deterministic (non-random) but not known [31]. We investigate a system consisting of a network of low-cost radiation counters (such as Geiger-Müller) which collaboratively operate to detect the presence of the radioactive source. Specifically, when the source is present, each sensor records an (unknown) emitted Poisson-distributed radiation count with a rate decreasing with the (unknown) sensor-source distance, according to a known Intensity Attenuation Function (IAF), embedded in a known Poisson background and Gaussian measurement noise. Each node transmits a single bit version to a FC, over noisy reporting channels (modelled as Binary Symmetric Channels, BSCs, and emulating low-energy communications), having the task of a global (more accurate) decision output. The FC employs the Generalized LOD (G-LOD) test [31, 32] as a lower-complexity alternative to GLRT, and a *novel* quantizer threshold design is proposed herein, based on a *heuristic rationale* developed resorting to the performance of Position-Clairvoyant (PC) LOD in asymptotic form. The resulting design is *sensor-individual*, considers the channel status between each sensor

and the FC, and depends upon neither the source intensity nor its position, thus allowing *offline* computation. Finally, numerical results provide a comparison of the aforementioned rules (while determining the performance drop with respect to PC LOD) vs. the sensor thresholds and test our design in a radioactive source scenario.

The paper organization is the following: Sect. 2 states the considered problem; Sect. 3 develops GLR and G-LOD tests for the considered problem; then, in Sect. 4 we focus on optimization of the quantizer; numerical results are reported and discussed in Sect. 5; finally, concluding remarks (with a mention to further avenues of research) are provided in Sect. 6.

*List of commonly-employed notations* - bold letters in lower-case indicate vectors, with  $a_n$  representing the  $n$ th component of  $\mathbf{a}$ ;  $\mathbb{E}\{\cdot\}$  and  $(\cdot)^T$  are the expectation and transpose operators, respectively; the unit (Heaviside) step function is denoted with  $p(\cdot)$  and  $P(\cdot)$  differentiate probability density functions (pdf) and probability mass functions (pmf), respectively; we denote a Gaussian pdf having mean  $\mu$  and variance  $\sigma^2$  with  $\mathcal{N}(\mu, \sigma^2)$  is used to;  $\mathcal{Q}(\cdot)$  (resp.  $p_{\mathcal{N}}(\cdot)$ ) denotes the complement of the cumulative distribution function (resp. the pdf) of a normal random variable in its standard form, i.e.  $\mathcal{N}(0, 1)$ ; finally, the symbol  $\sim$  (resp.  $\stackrel{a}{\sim}$ ) corresponds to “distributed as” (resp. to “asymptotically distributed as”).

## 2 Problem Statement

We focus on a binary test of hypotheses in which a set of nodes  $k \in \mathcal{K} \triangleq \{1, \dots, K\}$  is displaced to monitor a given area to decide the absence ( $\mathcal{H}_0$ ) or presence ( $\mathcal{H}_1$ ) of a radioactive source with an isotropic radiation pattern, incompletely-specified spatial signature, and intensity attenuation depending on the sensor-source distance, namely:

$$\begin{cases} \mathcal{H}_0 : & z_k = b_k + w_k \\ \mathcal{H}_1 : & z_k = c_k + b_k + w_k \end{cases}, \quad (1)$$

where  $z_k \in \mathbb{R}$  is the observation of  $k$ th sensor and  $w_k \sim \mathcal{N}(0, \sigma_{w,k}^2)$  is the measurement noise. In view of the spatial separation of the sensors, we hypothesize that the contribution due to noise terms  $w_k$ s are statistically independent. On the other hand, the terms  $b_k$  and  $c_k$  denote the background and the source radiation counts, respectively. More specifically, the radiation count of the background is assumed to obey a Poisson distribution with a rate  $\lambda_b$  (*known*), independent of  $w_k$ . Similarly, the count of source radiation at  $k$ th sensor is assumed to follow a Poisson law with parameter  $\lambda_{c,k}$ , and can be expressed through the parametric form

$$\lambda_{c,k}(\theta, \mathbf{x}_T) = \theta g^2(\mathbf{x}_T, \mathbf{x}_k) \triangleq \frac{\theta}{1 + \|\mathbf{x}_T - \mathbf{x}_k\|^2}, \quad (2)$$

where  $\theta$  denotes the source intensity, here assumed *unknown* (which well suits a realistic scenario) and *deterministic*, and  $g^2(\mathbf{x}_T, \mathbf{x}_k)$  has the meaning of an

IAF. In this work,  $\mathbf{x}_T \in \mathbb{R}^d$  is employed to denote the *unknown* source position, whereas  $\mathbf{x}_k \in \mathbb{R}^d$  refers to the *known* position of  $k$ th sensor, with the couple  $(\mathbf{x}_T, \mathbf{x}_k)$  giving the value of  $g(\mathbf{x}_T, \mathbf{x}_k)$ , being the IAF modelling the considered radioactive source.

Literature has shown that the considered signal model is well approximated with a Gaussian pdf [24], based on the Central Limit Theorem. Accordingly, we have:

$$\begin{cases} z_k | \mathcal{H}_0 \sim \mathcal{N}(\lambda_b, \lambda_b + \sigma_{w,k}^2) \\ z_k | \mathcal{H}_1 \sim \mathcal{N}(\lambda_{c,k}(\mathbf{x}_T) + \lambda_b, \lambda_{c,k}(\mathbf{x}_T) + \lambda_b + \sigma_{w,k}^2) \end{cases}, \quad (3)$$

Then, to cope with stringent energy and bandwidth budgets in realistic IoT scenarios, the  $k$ th sensor quantizes  $z_k$  within one bit of information, i.e.  $d_k \triangleq u(z_k - \tau_k)$ ,  $k \in \mathcal{K}$ , where  $\tau_k$  represents the quantizer threshold. For the sake of simplicity, we confine the focus of this paper to deterministic quantizers; the use and the analysis of the more general stochastic quantizers falls out the scope of our paper and left for future studies. Additionally, with the aim of modeling a reporting phase with constrained energy, we assume that  $k$ th sensor bit  $d_k$  is transmitted over a BSC and the FC, due to non-ideal transmission, observes an error-prone form  $\hat{d}_k = d_k$  (resp.  $\hat{d}_k = (1 - d_k)$ ) with probability  $(1 - P_{e,k})$  (resp.  $P_{e,k}$ ), which are here collected within  $\hat{\mathbf{d}} \triangleq [\hat{d}_1 \cdots \hat{d}_K]^T$ . In this paper  $P_{e,k}$  represents the bit-error probability of  $k$ th link, assumed known.

In view of the aforementioned assumptions, the bit probability under  $\mathcal{H}_1$  is given by

$$\alpha_k(\theta, \mathbf{x}_T) \triangleq (1 - P_{e,k})\beta_k(\theta, \mathbf{x}_T) + P_{e,k}(1 - \beta_k(\theta, \mathbf{x}_T)), \quad (4)$$

where  $\beta_k(\theta, \mathbf{x}_T) \triangleq \mathcal{Q}([\tau_k - \lambda_b - \theta g(\mathbf{x}_T, \mathbf{x}_k)]^2 / \sqrt{\sigma_{w,k}^2 + \lambda_b + \theta g(\mathbf{x}_T, \mathbf{x}_k)^2})$ . On the other hand, the bit probability under  $\mathcal{H}_0$  is obtained as  $\alpha_{k,0} \triangleq \alpha_k(\theta = 0, \mathbf{x}_T)$  (see Eq. (4)), thus giving:

$$\alpha_{k,0} = (1 - P_{e,k})\beta_{k,0} + P_{e,k}(1 - \beta_{k,0}), \quad (5)$$

where  $\beta_{k,0} \triangleq \mathcal{Q}([\tau_k - \lambda_b] / \sqrt{\lambda_b + \sigma_{w,k}^2})$ .

We highlight that the *unknown* source position  $\mathbf{x}_T$  can be *observed* at FC *only* when the expected intensity  $\theta > \theta_0$  ( $\theta_0 \triangleq 0$ ). Thus, we cast the problem as a *one-sided test where parameters of nuisance ( $\mathbf{x}_T$ ) are observable only under  $\mathcal{H}_1$*  [32], where  $\{\mathcal{H}_0, \mathcal{H}_1\}$  corresponds to  $\{\theta = \theta_0, \theta > \theta_0\}$ . The objective of our study is tantamount to a simple test derivation (from a computational standpoint) deciding in favour of  $\mathcal{H}_0$  (resp.  $\mathcal{H}_1$ ) when the statistic  $\Lambda(\hat{\mathbf{d}})$  is below (resp. above) the threshold  $\gamma_{fc}$ , and the design of the quantizer (i.e. an optimized  $\tau_k$ ,  $k \in \mathcal{K}$ ) for each sensor.

We evaluate the system performance of the FC adopting the generic decision statistic  $\Lambda$  through the detection ( $P_D \triangleq \Pr\{\Lambda > \gamma_{fc} | \mathcal{H}_1\}$ ) and false alarm ( $P_F \triangleq \Pr\{\Lambda > \gamma_{fc} | \mathcal{H}_0\}$ ) probabilities, respectively.

### 3 Fusion Rules

The GLR represents a widespread technique for composite hypothesis testing [29], and its implicit form is given by

$$\Lambda_{\text{GLR}}(\hat{\mathbf{d}}) \triangleq 2 \ln \left[ \frac{P(\hat{\mathbf{d}}; \hat{\theta}_1, \hat{\mathbf{x}}_T)}{P(\hat{\mathbf{d}}; \theta_0)} \right], \quad (6)$$

where  $P(\hat{\mathbf{b}}; \theta, \mathbf{x}_T)$  represents the likelihood as a function of  $(\theta, \mathbf{x}_T)$ . On the other hand,  $(\hat{\theta}_1, \hat{\mathbf{x}}_T)$  are the *Maximum Likelihood* (ML) *estimates* under  $\mathcal{H}_1$ , i.e.

$$(\hat{\theta}_1, \hat{\mathbf{x}}_T) \triangleq \arg \max_{(\theta, \mathbf{x}_T)} P(\hat{\mathbf{d}}; \theta, \mathbf{x}_T), \quad (7)$$

with  $\ln P(\hat{\mathbf{d}}; \theta, \mathbf{x}_T)$  being the logarithm of the likelihood function as a function of  $(\theta, \mathbf{x}_T)$ , whose explicit form is [29, 31]

$$\sum_{k=1}^K \left\{ \hat{d}_k \ln [\alpha_k(\theta, \mathbf{x}_T)] + (1 - \hat{d}_k) \ln [1 - \alpha_k(\theta, \mathbf{x}_T)] \right\}, \quad (8)$$

and an analogous expression holds for  $\ln P(\hat{\mathbf{d}}; \theta_0)$  by replacing the term  $\alpha_k(\theta, \mathbf{x}_T)$  with  $\alpha_{k,0}$ .

It is clear from Eq. (6) that  $\Lambda_{\text{GLR}}$  requires an optimization problem to be tackled. Sadly, an explicit expression for the couple  $(\hat{\theta}_1, \hat{\mathbf{x}}_T)$  is not available. This increases GLR computational complexity, usually involving an *approach based on grid discretization* on  $(\theta, \mathbf{x}_T)$ , see e.g. [29].

On the other hand, Davies' work represents an alternative approach for capitalizing the one-sided nature of the considered hypothesis test [32], allowing to generalize score-based tests to the more challenging scenario of nuisance parameters observed only under  $\mathcal{H}_1$ . In fact, score tests are based on ML estimates of nuisances under  $\mathcal{H}_0$  [27], that sadly cannot be obtained, because they are not *observable* in our case. In detail, if  $\mathbf{x}_T$  were available, the LOD would represent an effective, yet simple, fusion statistic for the corresponding problem testing a one-sided hypothesis [27]. Unfortunately, since  $\mathbf{x}_T$  is not known in the present setup, we rather obtain a *LOD statistics family* by varying such parameter. Such technical difficulty is overcome by Davies through the use of the *maximum of the family* as the decision statistic, that is:

$$\Lambda_{\text{GLOD}}(\hat{\mathbf{d}}) \triangleq \max_{\mathbf{x}_T} \frac{\left. \frac{\partial \ln [P(\hat{\mathbf{d}}; \theta, \mathbf{x}_T)]}{\partial \theta} \right|_{\theta=\theta_0}}{\sqrt{I(\theta_0, \mathbf{x}_T)}}, \quad (9)$$

where  $I(\theta, \mathbf{x}_T) \triangleq \mathbb{E} \left\{ \left( \frac{\partial \ln [P(\hat{\mathbf{d}}; \theta, \mathbf{x}_T)]}{\partial \theta} \right)^2 \right\}$  represents the Fisher Information (FI) assuming  $\mathbf{x}_T$  *known*. Henceforth, the above decision test will be referred to as *Generalized LOD* (G-LOD), to highlight the usage of LOD as the basic

statistic within the umbrella proposed by Davies [31]. The closed form of  $\Lambda_{\text{GLOD}}$  is drawn resorting to the explicit forms of the score function and the FI, as stated via the following corollaries, whose proof is omitted for brevity.

**Corollary 1.** *The score function  $\partial \ln [P(\hat{\mathbf{d}}; \theta, \mathbf{x}_T)] / \partial \theta$  for the considered radioactive source model is given explicitly as:*

$$\begin{aligned} \frac{\partial \ln [P(\hat{\mathbf{d}}; \theta, \mathbf{x}_T)]}{\partial \theta} &= \sum_{k=1}^K \left\{ (1 - 2P_{e,k}) g^2(\mathbf{x}_T, \mathbf{x}_k) p_{\mathcal{N}} \left( \frac{\tau_k - \lambda_b - \theta g^2(\mathbf{x}_T, \mathbf{x}_k)}{\sqrt{\sigma_{w,k}^2 + \lambda_b + \theta g^2(\mathbf{x}_T, \mathbf{x}_k)}} \right) \right. \\ &\quad \left. \times \frac{2\sigma_{w,k}^2 + \lambda_b + \theta g^2(\mathbf{x}_T, \mathbf{x}_k) + \tau_k}{2(\sigma_{w,k}^2 + \lambda_b + \theta g^2(\mathbf{x}_T, \mathbf{x}_k))^{3/2}} \right\} \end{aligned} \quad (10)$$

*Proof.* The proof can be obtained analogously as [31] by exploiting in the derivative calculation the separable form expressed by Eq. (8).

**Corollary 2.** *The FI  $I(\theta, \mathbf{x}_T)$  for the considered radioactive source model has the following closed form:*

$$I(\theta, \mathbf{x}_T) = \sum_{k=1}^K \psi_k(\theta, \mathbf{x}_T) g^4(\mathbf{x}_T, \mathbf{x}_k), \quad (11)$$

where the following auxiliary notation has been employed

$$\begin{aligned} \psi_k(\theta, \mathbf{x}_T) &\triangleq \frac{(1 - 2P_{e,k})^2}{\alpha_k(\theta, \mathbf{x}_T) [1 - \alpha_k(\theta, \mathbf{x}_T)]} \\ &\times \frac{\left\{ 2\sigma_{w,k}^2 + \lambda_b + \theta g^2(\mathbf{x}_T, \mathbf{x}_k) + \tau_k \right\}^2}{4(\sigma_{w,k}^2 + \lambda_b + \theta g^2(\mathbf{x}_T, \mathbf{x}_k))^3} p_{\mathcal{N}}^2 \left( \frac{\tau_k - \lambda_b - \theta g(\mathbf{x}_T, \mathbf{x}_k)^2}{\sqrt{\sigma_{w,k}^2 + \lambda_b + \theta g(\mathbf{x}_T, \mathbf{x}_k)^2}} \right). \end{aligned} \quad (12)$$

*Proof.* The proof can be obtained analogously as [31], exploiting conditional independence of decisions (which implies an additive form for the FI) and similar derivation results as  $\frac{\partial \ln [P(\hat{\mathbf{d}}; \theta, \mathbf{x}_T)]}{\partial \theta}$ .

Then, combining the results in (10) and (11), the G-LOD statistic is obtained in the final form as

$$\Lambda_{\text{GLOD}}(\hat{\mathbf{d}}) \triangleq \max_{\mathbf{x}_T} \Lambda_{\text{LOD}}(\hat{\mathbf{d}}, \mathbf{x}_T), \quad (13)$$

where

$$\Lambda_{\text{LOD}}(\hat{\mathbf{d}}, \mathbf{x}_T) = \frac{\sum_{k=1}^K \hat{\nu}_k(\hat{d}_k) g^2(\mathbf{x}_T, \mathbf{x}_k)}{\sqrt{\sum_{k=1}^K \psi_{k,0} g^4(\mathbf{x}_T, \mathbf{x}_k)}}, \quad (14)$$

is the LOD statistic when  $\mathbf{x}_T$  is assumed known, and we have employed  $\hat{\nu}_k(\hat{d}_k) \triangleq (\hat{d}_k - \alpha_{k,0}) \Xi_k$ ,  $\psi_{k,0} \triangleq \alpha_{k,0} (1 - \alpha_{k,0}) \Xi_k^2$  and

$$\Xi_k \triangleq \frac{(1 - 2P_{e,k}) \left[ 2\sigma_{w,k}^2 + \lambda_b + \tau_k \right]}{\alpha_{k,0} (1 - \alpha_{k,0}) 2(\sigma_{w,k}^2 + \lambda_b)^{3/2}} p_{\mathcal{N}} \left( \frac{\tau_k - \lambda_b}{\sqrt{\sigma_{w,k}^2 + \lambda_b}} \right), \quad (15)$$

as compact auxiliary definitions. We motivate the attractiveness of G-LOD with a *lower* (resp. a *simpler*) *complexity* (resp. *implementation*), as we do not require  $\hat{\theta}_1$ , and only a grid search with respect to  $\mathbf{x}_T$  is imposed, that is

$$\Lambda_{\text{GLOD}}(\hat{\mathbf{d}}) \approx \max_{i=1, \dots, N_{x_T}} \Lambda_{\text{LOD}}(\hat{\mathbf{d}}, \mathbf{x}_T[i]). \quad (16)$$

Hence, the complexity of its implementation scales as  $\mathcal{O}(K N_{x_T})$ , which implies a *significant reduction of complexity* with respect to the GLR (corresponding to  $\mathcal{O}(K N_{x_T} N_\theta)$ ).

It is evident that  $\Lambda_{\text{GLOD}}$  (the same applies to  $\Lambda_{\text{GLR}}$ , see Eqs. (6) and (14)) depends on  $\tau_k$  (via the terms  $\hat{\nu}_k(\hat{d}_k)$  and  $\psi_{k,0}$ ,  $k \in \mathcal{K}$ , (the threshold set is gathered within  $\boldsymbol{\tau} \triangleq [\tau_1 \cdots \tau_K]^T$ ) which can be *designed* to optimize performance. Accordingly, in Sect. 4 we accomplish this purpose.

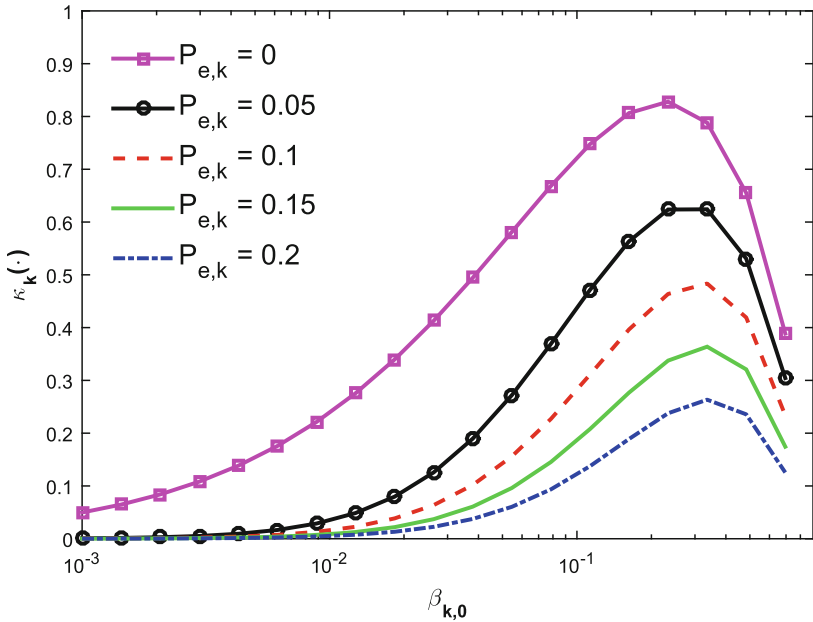


**Fig. 1.** Sensor threshold optimization: objective function  $\kappa_k(\beta_{k,0})$  is illustrated for sensor parameters  $(\sigma_{w,k}^2, \lambda_b) = (1, 1)$  and different  $P_{e,k}$  values.

## 4 Design of Quantizers

We point out that the rationale in [16,33] cannot be applied to design (asymptotically-) optimal deterministic quantizers, since no closed-form performance expressions exist for tests built upon Davies approach [32]. In view of this

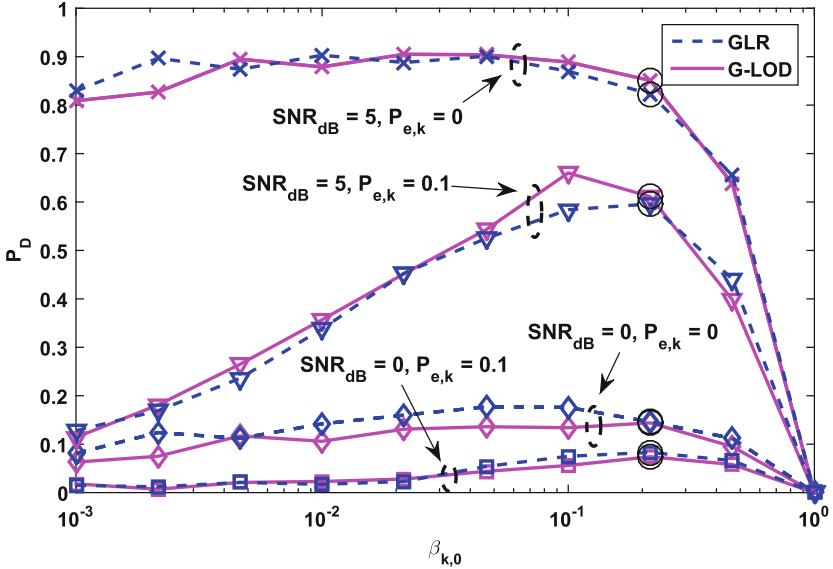


**Fig. 2.**  $P_D$  vs.  $\beta_{k,0} = \beta_0$ , when the FC false-alarm probability is set to  $P_F = 0.01$ . A WSN with  $K = 100$  sensors, having sensing  $\text{SNR} \in \{0, 5\}$  dB, is considered. Corresponding decisions are sent over BSCs with  $P_{e,k} \in \{0, 0.1\}$ . Circled markers correspond to (optimized)  $P_D(\tau^*)$ .

reason, we use a *modified rationale with respect to* [16, 33] (that is resorting to a heuristic, yet intuitive, basis) and demonstrate its effectiveness in Sect. 5 through simulations, as done for uncooperative target detection problems in [15, 34]. In detail, it is well known that the (position  $\mathbf{x}_T$ ) clairvoyant LOD statistic  $A_{\text{LOD}}$  is distributed (under an asymptotic, weak-signal, assumption<sup>1</sup>) as [27]

$$A_{\text{LOD}}(\mathbf{x}_T, \boldsymbol{\tau}) \underset{a}{\sim} \begin{cases} \mathcal{N}(0, 1) & \text{under } \mathcal{H}_0 \\ \mathcal{N}(\delta_Q(\mathbf{x}_T, \boldsymbol{\tau}), 1) & \text{under } \mathcal{H}_1 \end{cases}, \quad (17)$$

where the deflection<sup>2</sup>  $\delta_Q(\mathbf{x}_T, \boldsymbol{\tau}) \triangleq (\theta_1 - \theta_0) \sqrt{\text{I}(\theta_0, \mathbf{x}_T, \boldsymbol{\tau})}$  (underlining dependence on  $\mathbf{x}_T$  and  $\boldsymbol{\tau}$ ) is given as:

$$\delta_Q(\mathbf{x}_T, \boldsymbol{\tau}) = \theta_1 \sqrt{\sum_{k=1}^K \psi_{k,0}(\tau_k) g^4(\mathbf{x}_T, \mathbf{x}_k)}, \quad (18)$$

with  $\theta_1$  representing the *true value* when  $\mathcal{H}_1$  holds true. Obviously, the higher  $\delta_Q(\mathbf{x}_T, \boldsymbol{\tau})$ , the better the performance for the  $\mathbf{x}_T$ -clairvoyant LOD test is

<sup>1</sup> That is  $|\theta_1 - \theta_0| = c/\sqrt{K}$  for a certain value  $c > 0$  [27].

<sup>2</sup> By doing a slight notation abuse, we adopt the notation  $\text{I}(\theta, \mathbf{x}_T, \boldsymbol{\tau})$  (resp.  $\psi_{k,0}(\tau_k)$  and  $\beta_{k,0}(\tau_k)$ ) in the place of  $\text{I}(\theta, \mathbf{x}_T)$  (resp.  $\psi_{k,0}$  and  $\beta_{k,0}$ ) to highlight their parametric dependence on the local thresholds  $\tau_k$ 's.

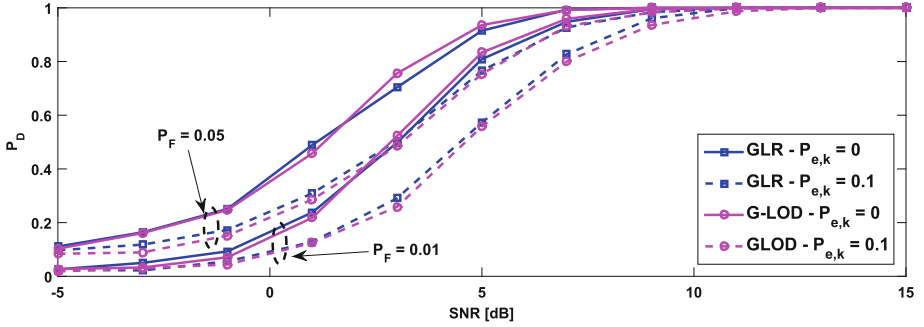


**Fig. 3.**  $P_D$  vs. sensing SNR (dB), when the FC false-alarm probability is set to  $P_F \in \{0.05, 0.01\}$ . A WSN with  $K = 100$  sensors is considered, with sensor thresholds set as  $\tau_k = \tau_k^*$  and whose decisions are sent over BSCs with  $P_{e,k} = P_e \in \{0, 0.1\}$

expected to perform in a one-sided test which assumes that the source to be revealed is placed at  $\mathbf{x}_T$ . We highlight that, for one-sided testing, no immediate expressions in the literature are found for GLRT in the asymptotic case [27]. Nonetheless, for the sake of a complete comparison, our proposed design will be also applied to the GLRT in the numerical results later reported in Sect. 5.

For the mentioned reasons, we design vector of thresholds  $\boldsymbol{\tau}$  to maximize  $\delta_Q(\mathbf{x}_T, \boldsymbol{\tau})$ , namely

$$\boldsymbol{\tau}^* \triangleq \arg \max_{\boldsymbol{\tau}} \delta_Q(\mathbf{x}_T, \boldsymbol{\tau}) \quad (19)$$

In the general case such approach would imply a  $\boldsymbol{\tau}^*$  which depends on  $\mathbf{x}_T$  (hence not practical). Still, for this particular problem, the optimization requires only the solution of  $K$  *decoupled* threshold designs (hence the optimization complexity presents a linear scale with the number of sensors  $K$ ), being also *independent of*  $\mathbf{x}_T$  (cf. Eq. (18)), that is:

$$\max_{\tau_k} \left\{ \psi_{k,0}(\tau_k) = \frac{(2\sigma_{w,k}^2 + \lambda_b + \tau_k)^2}{4[\sigma_{w,k}^2 + \lambda_b]^3} \frac{p_{\mathcal{N}}^2([\tau_k - \lambda_b]/\sqrt{\sigma_{w,k}^2 + \lambda_b})}{\Delta_k + \beta_{k,0}(\tau_k)[1 - \beta_{k,0}(\tau_k)]} \right\}, \quad (20)$$

where  $\Delta_k \triangleq [P_{e,k}(1 - P_{e,k})]/(1 - 2P_{e,k})^2$ . Examples of the objective  $\psi_{k,0}(\tau_k)$  for a number of  $P_{e,k}$  (or, equivalently,  $\Delta_k$ ) values are illustrated in Fig. 1. We reformulate such maximization (being in *bijective* correspondence with  $\tau_k$  through the relationship  $\tau_k = \mathcal{Q}^{-1}(\beta_{k,0})\sqrt{\lambda_b + \sigma_{w,k}^2} + \lambda_b$ ), as

$$\kappa_k(\beta_{k,0}) = \frac{p_{\mathcal{N}}^2(\mathcal{Q}^{-1}(\beta_{k,0})) \left[ 1 + \frac{1}{2}\mathcal{Q}^{-1}(\beta_{k,0})/\sqrt{\sigma_{w,k}^2 + \lambda_b} \right]^2}{\Delta_k + \beta_{k,0}(1 - \beta_{k,0})} \quad (21)$$

Examples of the objective  $\kappa_k(\beta_{k,0})$  for a number of  $P_{e,k}$  (viz.  $\Delta_k$ ) values are illustrated in Fig. 1. Therefore, we can evaluate the optimized  $\tau_k^*$  (viz.  $\beta_{k,0}^*$ ) via a simple numerical search on a 1-D grid.

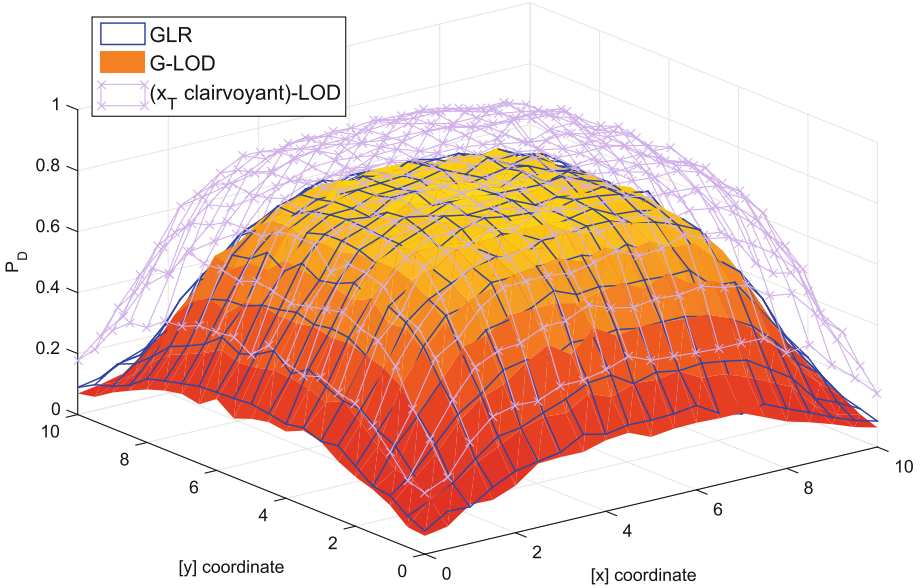


**Fig. 4.** Profile of  $P_D$  vs. source position  $\mathbf{x}_T$ , when the FC false-alarm probability is set to  $P_F = 0.01$ . A WSN with  $K = 100$  sensors, having sensing SNR = 5 dB, is considered. Corresponding decisions are sent over BSCs with  $P_{e,k} = 0.1$ . Finally,  $\beta_{k,0}$ 's are selected to maximize Eq. (21).

## 5 Numerical Results

Henceforth we delve into performance investigation of both tests and we assess the threshold-optimization developed in Sect. 4. With this aim, a 2-D area ( $\mathbf{x}_T \in \mathbb{R}^2$ ) is considered, in which the presence of a radioactive source in the surveillance region  $\mathcal{A} \triangleq [0, 10]^2$  (i.e. a square) is monitored by a WSN composed of  $K = 100$  sensor nodes. For the sake of a simplicity, we arrange sensors on a uniform square grid which covers the whole  $\mathcal{A}$ . Regarding the model assumptions for the sensing phase, we hypothesize  $w_k \sim \mathcal{N}(0, \sigma_w^2)$ ,  $k \in \mathcal{K}$  and, for simplicity, we set  $(\sigma_w^2, \lambda_b) = (1, 1)$ . Lastly, we define  $\text{SNR} \triangleq 10 \log_{10}[\theta/(\sigma_w^2 + \lambda_b)]$  the source Signal-To-Noise Ratio (SNR), to measure the strength of the radioactive source to be detected.

According to Sect. 3, the implementation of  $\Lambda_{\text{GLR}}$  and  $\Lambda_{\text{GLOD}}$  resorts to search on grids for  $\theta$  and  $\mathbf{x}_T$ . First, the search space of  $\theta$  is constrained within  $S_\theta \triangleq [0, \theta]$ , where  $\theta > 0$  corresponds to  $\text{SNR} = 20$  dB. The vector collecting the points on the grid is then defined as  $[0 \ \mathbf{g}_\theta^T]^T$ , with  $\mathbf{g}_\theta$  including the intensity values which correspond to the sampling of the SNR (dB)  $-10 : 2.5 : 20$  (leading to  $N_\theta = 12$ ). Secondly, the search support of  $\mathbf{x}_T$  is naturally assumed to be coincident with the monitored area, i.e.  $S_{\mathbf{x}_T} = \mathcal{A}$ . Accordingly, the 2-D grid is the result of sampling  $\mathcal{A}$  uniformly with  $N_{\mathbf{x}_T} = N_c^2$  points, where  $N_c = 100$ .

In this setup, the evaluation of G-LOD requires  $N_c^2 = 10^4$  grid points, as opposed to  $N_c^2 N_\theta = 1.2 \times 10^5$  points for GLR, i.e. a *more than tenfold complexity decrease*.

Initially, in Fig. 2 we report  $P_D$  (under  $P_F = 0.01$ ,  $\text{SNR} \in \{0, 5\}$  dB and  $P_{e,k} \in \{0, 0.1\}$ ) vs. the same *local* (sensor) bit-activation probability  $\beta_{k,0} = \beta_0$ ,  $k \in \mathcal{K}$  (enforced via a common threshold choice) so as to assess sensitivity w.r.t. sensor quantizer threshold. At each run, the source position  $\mathbf{x}_T$  is drawn randomly based on a *uniformly-distributed pdf* within the region  $\mathcal{A}$ . The optimized threshold  $\tau_k^*$  (viz.  $\beta_{k,0}^*$ ) proposed in Sect. 4 apparently represents a solution of appealing (circled markers highlight the corresponding  $P_D$ ), since the optimal  $P_D$  of each curve is a function on the (*unknown*) source SNR measured, and since a naively chosen  $\beta_0$  may imply a high performance loss. This reasoning *also* applies to the GLR.

Then, in Fig. 3 we provide a  $P_D$  comparison (for  $P_F \in \{0.05, 0.01\}$ ) of considered rules (for a source whose position is randomly generated within  $\mathcal{A}$  at each run, similarly as Fig. 2) versus SNR (dB), in order to assess their detection sensitivity as a function of the dispersion strength of the radioactive source. From inspection of the figure, we concluded that both rules perform very similarly for a different quality of the BSC ( $P_{e,k} = P_e \in \{0, 0.1\}$ ) and over the whole SNR range.

Thirdly, in Fig. 4, we report  $P_D$  (under  $P_F = 0.01$ ) profile vs. source location  $\mathbf{x}_T$  (for  $\text{SNR} = 5$  dB,  $P_{e,k} = 0.1$  and optimized  $\beta_{k,0}^*$ ), to draw a detailed overview of detection capabilities over the whole monitored area  $\mathcal{A}$  and underline possibly *blind spots*. Remarkably, G-LOD test performs only *negligibly worse* than the GLRT, and moderately worse in comparison to a test based on PC LOD (given in Eq. (14), having an  $\mathcal{O}(K)$  complexity). Unfortunately, the latter assumes *the unrealistic* knowledge of  $\mathbf{x}_T$  and thus merely constitutes an *upper-limiting bound* on performance achievable. Finally, we notice that both rules have a similar  $P_D(\mathbf{x}_T)$  profile, and its “shape” highlights a lower detection rate at the edge of the monitored area. Such result can be ascribed to the *regularity* of the WSN arrangement in the monitored area  $\mathcal{A}$ .

## 6 Concluding Remarks and Further Directions

In this paper, a distributed scheme using a WSN for detection of a nuclear radioactive source was developed. More specifically, we considered a source emitting an unknown intensity ( $\theta$ ) at unknown position ( $\mathbf{x}_T$ ), as an alternative enjoying low-complexity as opposed to the GLRT (which, instead, requires a grid search within the space of  $(\theta, \mathbf{x}_T)$ ). Specifically, we generalized the LOD test, based on the rationale proposed by [32]. Furthermore, we developed an effective criterion (originating from performance expressions having a semi-theoretical background) to design sensor thresholds of G-LOD in an optimized fashion, resulting in a *sensor-individual (simple) numerical search on a 1-D grid*. Remarkably, we capitalized the obtained result so as to optimize both GLR and G-LOD tests performance. Numerical results underlined the close performance of G-LOD test to the GLRT in the scenarios investigated, and a small (yet reasonable) loss of GLOD compared to a test based on PC LOD. Our future work

will consist of investigating design of fusion rules in more challenging radioactive source scenarios, such as inhomogeneous radiation background, multiple moving sources and burstiness (time-correlation) of reporting channels.

## References

1. Jin, J., Gubbi, J., Marusic, S., Palaniswami, M.: An information framework for creating a smart city through Internet of Things. *IEEE Internet Things J.* **1**(2), 112–121 (2014)
2. Varshney, P.K.: *Distributed Detection and Data Fusion*, 1st edn. Springer, New York (1996). <https://doi.org/10.1007/978-1-4612-1904-0>
3. Coaffee, J., Moore, C., Fletcher, D., Boshier, L.: Resilient design for community safety and terror-resistant cities. In: *Proceedings of the Institution of Civil Engineers-Municipal Engineer*, vol. 161, pp. 103–110. Thomas Telford Ltd. (2008)
4. Brennan, S.M., Mielke, A.M., Torney, D.C., MacCabe, A.B.: Radiation detection with distributed sensor networks. *IEEE Comput.* **37**(8), 57–59 (2004)
5. Brennan, S.M., Mielke, A.M., Torney, D.C.: Radioactive source detection by sensor networks. *IEEE Trans. Nucl. Sci.* **52**(3), 813–819 (2005)
6. Stephens, D.L., Peurrung, A.J.: Detection of moving radioactive sources using sensor networks. *IEEE Trans. Nucl. Sci.* **51**(5), 2273–2278 (2004)
7. Pahlajani, C.D., Poulakakis, I., Tanner, H.G.: Networked decision making for Poisson processes with applications to nuclear detection. *IEEE Trans. Autom. Control* **59**(1), 193–198 (2014)
8. Pahlajani, C.D., Sun, J., Poulakakis, I., Tanner, H.G.: Error probability bounds for nuclear detection: improving accuracy through controlled mobility. *Automatica* **50**(10), 2470–2481 (2014)
9. Morelande, M., Ristic, B., Gunatilaka, A.: Detection and parameter estimation of multiple radioactive sources. In: *10th International Conference on Information Fusion (FUSION)*, pp. 1–7 (2007)
10. Morelande, M.R., Ristic, B.: Radiological source detection and localisation using Bayesian techniques. *IEEE Trans. Signal Process.* **57**(11), 4220–4231 (2009)
11. Ristic, B., Morelande, M., Gunatilaka, A.: Information driven search for point sources of gamma radiation. *Signal Process.* **90**(4), 1225–1239 (2010)
12. Hoballah, I.Y., Varshney, P.K.: Distributed Bayesian signal detection. *IEEE Trans. Inf. Theory* **35**(5), 995–1000 (1989)
13. Reibman, A.R., Nolte, L.W.: Optimal detection and performance of distributed sensor systems. *IEEE Trans. Aerosp. Electron Syst.* **1**, 24–30 (1987)
14. Viswanathan, R., Varshney, P.K.: Distributed detection with multiple sensors - part I: fundamentals. *Proc. IEEE* **85**(1), 54–63 (1997)
15. Ciunozzo, D., Salvo Rossi, P., Willett, P.: Generalized Rao test for decentralized detection of an uncooperative target. *IEEE Signal Process. Lett.* **24**(5), 678–682 (2017)
16. Fang, J., Liu, Y., Li, H., Li, S.: One-bit quantizer design for multisensor GLRT fusion. *IEEE Signal Process. Lett.* **20**(3), 257–260 (2013)
17. Ciunozzo, D., Salvo Rossi, P.: Decision fusion with unknown sensor detection probability. *IEEE Signal Process. Lett.* **21**(2), 208–212 (2014)
18. Aalo, V.A., Viswanathan, R.: Multilevel quantisation and fusion scheme for the decentralised detection of an unknown signal. *IEE Proc. Radar Sonar Navig.* **141**(1), 37–44 (1994)

19. Chen, B., Jiang, R., Kasetkasem, T., Varshney, P.K.: Channel aware decision fusion in wireless sensor networks. *IEEE Trans. Signal Process.* **52**(12), 3454–3458 (2004)
20. Ciunzo, D., Romano, G., Salvo Rossi, P.: Channel-aware decision fusion in distributed MIMO wireless sensor networks, decode-and-fuse vs. decode-then-fuse. *IEEE Trans. Wireless Commun.* **11**(8), 2976–2985 (2012)
21. Niu, R., Varshney, P.K.: Performance analysis of distributed detection in a random sensor field. *IEEE Trans. Signal Process.* **56**(1), 339–349 (2008)
22. Chin, J.R., et al.: Identification of low-level point radioactive sources using a sensor network. *ACM Trans. Sens. Netw. (TOSN)* **7**(3), 21 (2010)
23. Sen, S., et al.: Performance analysis of Wald-statistic based network detection methods for radiation sources. In: 19th International Conference on Information Fusion (FUSION), pp. 820–827 (2016)
24. Sundaresan, A., Varshney, P.K., Rao, N.S.V.: Distributed detection of a nuclear radioactive source using fusion of correlated decisions. In: 10th IEEE International Conference on Information Fusion (FUSION), pp. 1–7 (2007)
25. Sundaresan, A., Varshney, P.K., Rao, N.S.V.: Copula-based fusion of correlated decisions. *IEEE Trans. Aerosp. Electron. Syst.* **47**(1), 454–471 (2011)
26. Sundaresan, A., Varshney, P.K., Rao, N.S.V.: Distributed detection of a nuclear radioactive source based on a hierarchical source model. In: IEEE International Conference on Acoustics, Speech and Signal Processing (ICASSP), pp. 2901–2904 (2009)
27. Kay, S.M.: *Fundamentals of Statistical Signal Processing, Volume 2: Detection Theory*. Prentice Hall PTR, Upper Saddle River (1998)
28. Niu, R., Varshney, P.K.: Joint detection and localization in sensor networks based on local decisions. In: 40th Asilomar Conference on Signals, Systems and Computers, pp. 525–529 (2006)
29. Shoari, A., Seyedi, A.: Detection of a non-cooperative transmitter in Rayleigh fading with binary observations. In: IEEE Military Communications Conference (MILCOM), pp. 1–5 (2012)
30. Kailkhura, B., Ray, P., Rajan, D., Yen, A., Barnes, P., Goldhahn, R.: Byzantine-resilient locally optimum detection using collaborative autonomous networks. In: IEEE International Workshop on Computational Advances in Multi-Sensor Adaptive Processing (CAMSAP) (2018)
31. Ciunzo, D., Salvo Rossi, P.: Distributed detection of a non-cooperative target via generalized locally-optimum approaches. *Inf. Fusion* **36**, 261–274 (2017)
32. Davies, R.D.: Hypothesis testing when a nuisance parameter is present only under the alternative. *Biometrika* **74**(1), 33–43 (1987)
33. Ciunzo, D., Papa, G., Romano, G., Salvo Rossi, P., Willett, P.: One-bit decentralized detection with a Rao test for multisensor fusion. *IEEE Signal Process. Lett.* **20**(9), 861–864 (2013)
34. Ciunzo, D., Salvo Rossi, P.: Quantizer design for generalized locally optimum detectors in wireless sensor networks. *IEEE Wirel. Commun. Lett.* **7**(2), 162–165 (2018)